

Control of electromagnetic environment in smart traction power supply systems

Natalya Buyakova^{1,*}, Vasily Zakaryukin², and Andrey Kryukov^{2,3}

¹Angarsk State Technical University, ul. Chaykovskogo, 60, 665835, Angarsk, Russia

²Irkutsk State Transport University, ul. Chernyshevskogo, 15, 664074 Irkutsk, Russia

³Irkutsk national research technical university, st. Lermontova, 83, 664074 Irkutsk, Russia

Abstract. The possibility of reducing the intensity of magnetic field created by a traction network of an alternating current electrified railroad is considered in the article. The electric field of such a traction network at a height of 1,8 m above is relatively small. In order to control the electromagnetic situation, 2x25 kV traction systems, sucking transformers with a return wire for the 25 kV system, amplifying and shielding wires of the traction network, passive screens on passenger platforms, optimization of train traffic schedules can be used. Fazonord software package developed at the Irkutsk State Transport University was used as a tool for the analysis of the above events. Using computer simulations, it was shown that the most effective methods for reducing the magnetic field strength are the use of screens on passenger platforms, optimal train schedules, and the use of "soft" train driving modes. The latter measure is able to reduce the peak magnetic field strength by about 25%.

1 Introduction

The electromagnetic situation created by the traction power supply system determines the working conditions of the maintenance personnel, the effect of the electromagnetic field on the passengers of the railway transport, and the level of interference created by the traction network on adjacent devices. At the same time, the current stage in the development of the electric power industry is characterized by the transition to a new technological platform based on the smart grid concept [1]. The AC railway power supply system (RPSS) is a kind of three-phase single-phase network, to which this concept is applicable in full [2 - 9].

The implementation of the smart RPSS will improve the conditions of human electromagnetic security and reduce the level of interference created by a single-phase traction network.

Fazonord software package developed at the Irkutsk State Transport University [3, 10] was used as a working tool for analyzing the effectiveness of various methods for controlling the electromagnetic situation of the AC traction network. The package makes it possible to calculate the regime in the combined electrical system of external and traction

*Corresponding author: bn_900@mail.ru

power supply and to determine the electric and magnetic fields of multi-wire traction networks and transmission lines on the basis of the regime parameters. This approach differs from the classical methods [11 - 13], taking into account the specific regime of the system and the current distribution in the multi-wire traction network.

2 Structure of smart railway power supply system

The structure of smart RPSS (shown in fig. 1) includes the following blocks:

- digital complexes that monitor the condition of electrical equipment, including devices operating on-line;
- automatic control devices based on digital technologies;
- controlled reactive power sources implemented using the FACTS concept (flexible alternative current transmission system);
- distributed generation plants and energy storages;
- a set of devices for improving the quality of electricity.

3 Modeling method

Due to the relatively low voltage level in the traction network acting on the RPSS, the level of electric field strength at a standard height of 1,8 meters from the level of the railway track lies within the permissible limits. Therefore, below the problem of electromagnetic situation (EMS), control is considered only by the criterion of the magnetic field strength.

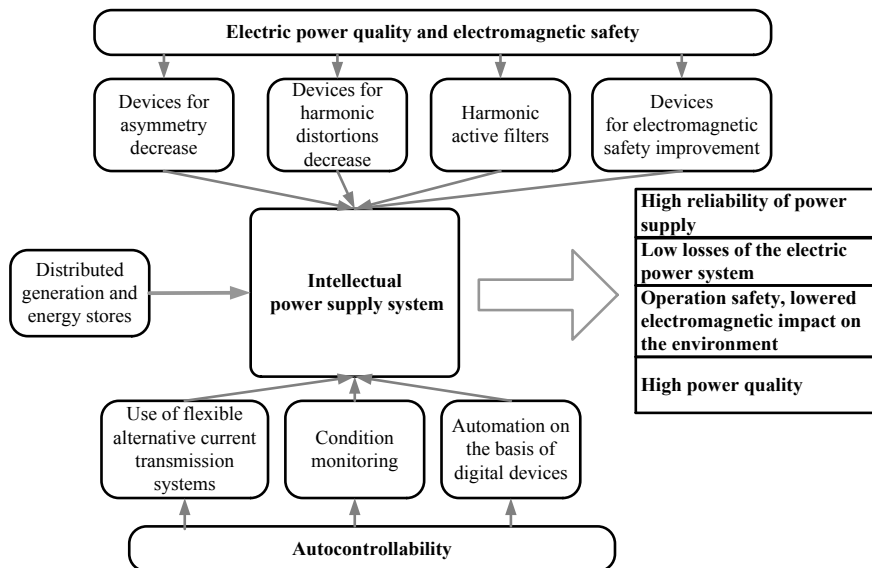


Fig. 1. Structure of smart railway power supply system.

The task of EE control can be formulated in a general way as follows:

$$\max \mathbf{H} \leq H_{DOP},$$

where $\mathbf{H} = \mathbf{H}_{MAX} [\mathbf{I}(t), \mathbf{K}^{(P)}, \mathbf{K}]$ – is the vector of the voltage values in the controlled points of the traction network space;

$\mathbf{H} = [H_1 \ H_2 \ \dots \ H_n]^T$; n – is the number of points at which the magnetic field strength is monitored (observed);

$\mathbf{I}(t)$ – is the vector of currents in the wires of the traction network, depending on time t ,

$$\mathbf{I}(t) = [I_1(t) \ I_2(t) \ \dots \ I_N(t)]^T;$$

N – is the number of wires of the traction network, including rails;

$\mathbf{K}^{(p)} = [x_1^{(p)} \ y_1^{(p)} \ \dots \ x_c^{(p)} \ y_c^{(p)}]^T$ – is the Cartesian vector of wires of the traction network; the reference point is located on the axis of the railway to the ground surface with the X axis of the right-sided system being perpendicular to the railway axis and directed along the ground surface, the Y axis being perpendicular to the ground surface, and the Z axis being directed along the railway axis against the accepted positive direction of the wire currents;

$\mathbf{K} = [x_1 \ y_1 \ x_2 \ y_2 \ \dots \ x_n \ y_n]^T$ – is the Cartesian vector of observation points.

The computation of the \mathbf{H} vector components for a specific time instant at a particular control point is carried out by the following formulas of a plane-parallel field:

$$\dot{H}_x = \frac{1}{2\pi} \sum_{i=1}^N \dot{I}_i \frac{y - y_i^{(p)}}{(x_i^{(p)} - x)^2 + (y_i^{(p)} - y)^2};$$

$$\dot{H}_y = -\frac{1}{2\pi} \sum_{i=1}^N \dot{I}_i \frac{x - x_i^{(p)}}{(x_i^{(p)} - x)^2 + (y_i^{(p)} - y)^2};$$

$$\dot{H}_z = 0.$$

After the transition from the integrated effective values of the components to the time dependences one can obtain the parametric equations of the vector hodograph of the electric field strength:

$$H_x(t) = \sqrt{2} H_x \sin(\omega t + \varphi_x);$$

$$H_y(t) = \sqrt{2} H_y \sin(\omega t + \varphi_y),$$

where the $\sqrt{2}$ factor is required due to the fact that voltage calculations are performed according to the actual values; $\omega = 314$ rad/s.

The maximum value H_{MAX} of the field strength reaches at the instants, determined by the following equation:

$$t_{max} = \frac{1}{2\omega} \text{Arctg} \frac{H_x^2 \sin 2\varphi_x + H_y^2 \sin 2\varphi_y}{H_x^2 \cos 2\varphi_x + H_y^2 \cos 2\varphi_y}.$$

One of the arc tangent values is chosen based on the condition of the negative value of the second derivative:

$$H_x^2 \cos 2(\omega t_{max} + \varphi_x) + H_y^2 \cos 2(\omega t_{max} + \varphi_y) < 0.$$

The effective value of the field strength along a certain direction Ψ , measured from the positive direction of the X axis, is equal to

$$H_{\Psi} = \sqrt{\frac{1}{2\pi} \int_0^{2\pi} 2\Theta^2 d(\omega t)},$$

$$\Theta = \Lambda_1 + \Lambda_2; \quad \Lambda_1 = H_x \cos \psi \sin(\omega t + \varphi_x);$$

$$\Lambda_2 = H_y \sin \psi \sin(\omega t + \varphi_y).$$

Then

$$H_{\Psi}^2 = \frac{1}{\pi} \int_0^{2\pi} [\Lambda_1^2 + \Lambda_2^2 + 2\Lambda_1\Lambda_2] d(\omega t);$$

$$H_{\Psi} = \sqrt{A^2 + B^2 + C};$$

$$A = H_x \cos \psi; \quad B = H_y \sin \psi;$$

$$C = 2H_x H_y \sin \psi \cos \psi \cos(\varphi_x - \varphi_y).$$

Extreme voltage values are calculated using the following formula:

$$H_{\Psi E} = [\Omega_1 \pm \Omega_2]^{\frac{1}{2}},$$

$$\Omega_1 = \frac{H_x^2 + H_y^2}{2};$$

$$\Omega_2 = \frac{\sqrt{(H_x^2 + H_y^2)^2 - 4H_x^2 H_y^2 \sin^2(\varphi_x - \varphi_y)}}{2}.$$

The plus sign corresponds to the maximum voltage, the minus sign - to the minimum voltage. This approach for determining the extreme values is presented in [14].

4 Measurement of electromagnetic situation

EMS control can be reduced to the task of decreasing the levels of magnetic field strength at given points of space, which surrounds the traction network. These methods are divided into two groups: technical and regime (fig. 2).

The following technical solutions can be assigned to the activities of the first group:

- 1) use of autotransformer 2-25 kV RPSS;
- 2) use of sucking transformers with return wire;
- 3) installation of amplifying and shielding wires;
- 4) use of passive screens installed on passenger platforms.

The activities of the second group include the following:

- 1) optimization of traffic schedules and regimes of driving trains by the criterion of improving the electromagnetic situation;

2) use of the automatic train operation systems with algorithms that include blocks aimed at reducing peak loads.

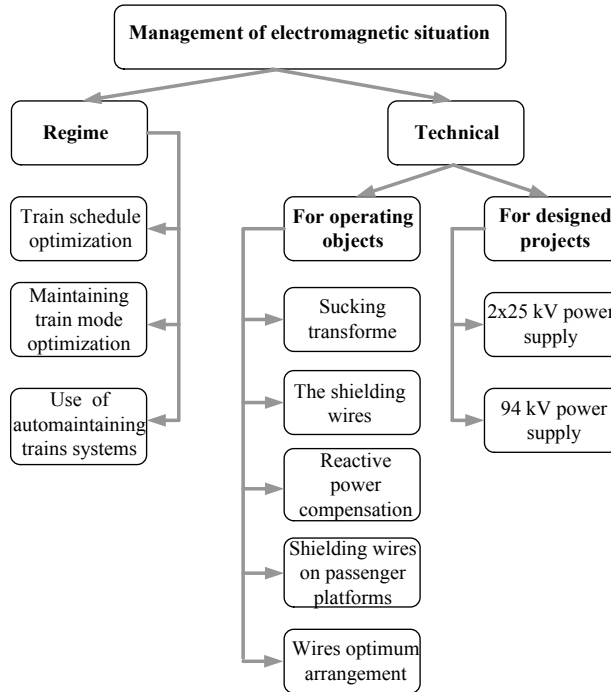


Fig. 2. Methods of electromagnetic situation management.

In order to reduce the EMF intensity levels directly on the passenger platforms of railway stations, the use of passive shields in the form of horizontal rods grounded on both sides of the track can be recommended. To analyze the screening effect, it is reasonable to consider the structure of the field of one platform in fig. 3.

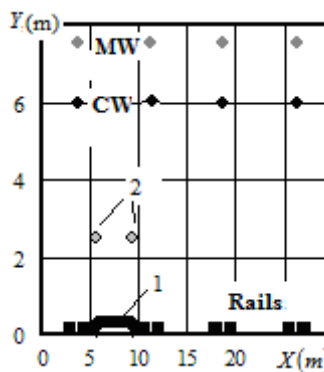


Fig. 3. Fragment of cross section of 8-way traction net with screens on passenger platform: 1– platform imitating wires; 2 – screen wires; CW –contact wire; MW – messenger wire.

In the model of the 2 km section, 16 wires of the contact network PBSM-95+MF-100 of the eight-way section were taken into account with two shielding wires with characteristics similar to those of the AC-70 wires, 16 P-65 rails and 124 conductors for simulating conductive grounded reinforcement of passenger platforms. Conductors of platform models

were assumed to be under zero potential, so their nodes are not clearly marked in the design model.

The design model included 16 models of impedance bonds, which allow correct determining of the currents of rails. Network calculations were carried out with total loads of contact networks of a $10 + j10$ MVA section for up and down directions.

Shielding wires (SWs) were located at points with coordinates X in fig. 3, equal to 5,5 m and 9,5 m. Two variants of grounding along the edges of the shielding wires were considered: separate grounding conductors with a resistance of 1 Ohm and taking into account their connection to the near rail. The results of EMF calculations at a height of 1,8 m at different arrangement altitudes of shielding wires using separate earthing switches are presented in table 1 and in fig. 4, 5.

Table 1. Amplitude maximum values when screens are earthed.

Indicator	Without SWs	SW suspension height, m			Difference, %		
		2,5	3,5	4	2 & 3	2 & 4	2 & 5
1	2	3	4	5	6	7	8
E_{MAX}	3,58	2,77	2,36	2,418	-22,6	-34,0	-32,4
	28,88	28,06	27,9	27,9	-2,8	-3,4	-3,4

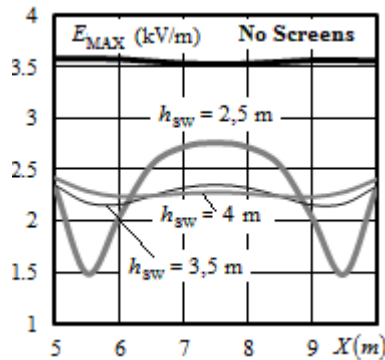


Fig. 4. Electric field amplitude when screens are earthed on separate earthing: h_{sw} – screen wire height.

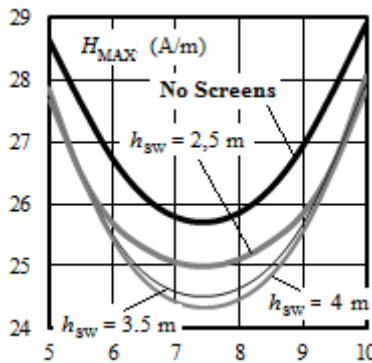


Fig. 5. Magnetic field amplitude when screens are earthed on separate earthing.

The results of calculations show that the use of shielding wires having separate earthing switches significantly reduces the electric field of the contact network, but has little effect

on the magnetic field. The connection of the screening wire to the nearest rail can be even more promising. Table 2 and fig. 6, 7 reflect the structure of the electromagnetic field at a height of 1,8 m with such a connection of shielding wires located at different heights.

For a variant without screens, similar magnetic field strengths reduced to the current unit of the contact network are given in the paper [15].

Table 2. Amplitude values at the middle of platform when screens are connected with rails.

Indicator	Without SWs	SW suspension height, m			Difference, %		
		2,5	3,5	4	2 & 3	2 & 4	2 & 5
1	2	3	4	5	6	7	8
E_{MAX}	3,58	2,77	2,36	2,42	-22,7	-34,1	-32,5
H_{MAX}	28,88	19,31	19,78	20,33	-33,2	-31,5	-29,6

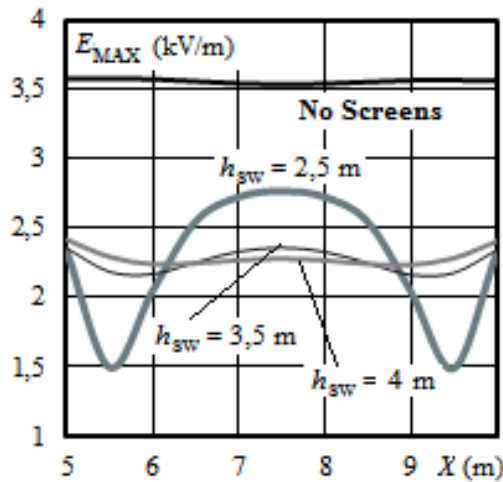


Fig. 6. Electric field amplitude when screens are connected with rail.

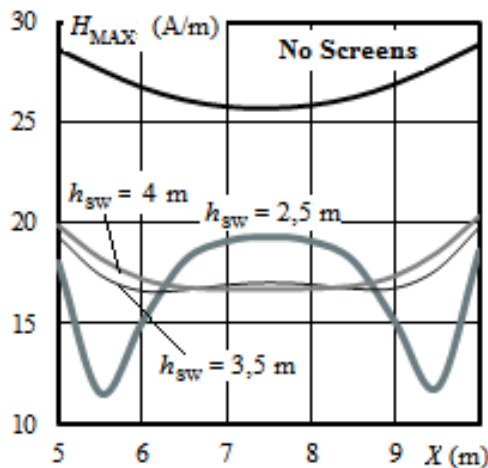


Fig. 7. Magnetic field amplitude when screens are connected with rail.

With respect to the electric field, the connection of the shielding wires to the rails makes practically no difference from the connection to separate earthing switches, but it reduces

the magnetic field strength in the middle of the platform with the height of the screening wire suspension 3 ... 4 m by about a third. In addition, the connection to the rail is much simpler during installation and does not introduce distortions into the operation of rail circuits, provided that the shielding wires are suspended on insulators. The difference of the screening effect with respect to the magnetic field for different ways of grounding the shielding wires is associated with significant differences in the currents in the shielding wires.

When grounding to separate earth conductors, only induced currents flow in the wires, and when grounding the rail itself, a part of the current of the rail branches off onto the rail; in the calculations the currents in the wires connected to the rail were about three times as large as in the other variant.

Another possibility to regulate the magnetic field of the traction network is to organize the optimal train schedule. Optimization of the schedule according to the criterion of minimum current loads of the contact network leads to minimization of the magnetic field strength of the traction network. The simplest solution can be the formation of a traffic schedule with alternating heavy trains with trains of small mass.

In order to study the effectiveness of this technology, an imitation simulation of the traction power system of a single-track section with a contact network PBSM-95+MF-100 was carried out. A section with two inter-station zones 30 km long and three traction transformers TDTNZh-4000/110 was considered.

To assess the possibilities of reducing current loads and magnetic field of the traction network two schedules for the movement of up trains were considered (with approximately equal volume of train operation):

- 1) bunch schedule with the same trains weighing 3,892 tons, inter-train interval 9 minutes, interval between bunches of trains 20 minutes;
- 2) movement of trains weighing 3,192 tons, 4,192 tons, 5,192 tons, inter-train intervals 9 minutes and 12 minutes, intervals between bunches of trains 14 minutes.

The results of the simulation are shown in fig. 8 and in table 3.

In comparison with the double-track section, the single-track section is characterized by lower EMF strengths and a faster decline when moving away from the axis of the railway. In general, the values of voltage are far from limiting, but the results show that optimization of the train schedule by the criterion of the permissible magnetic field strength can be used as an effective means of controlling the EMS.

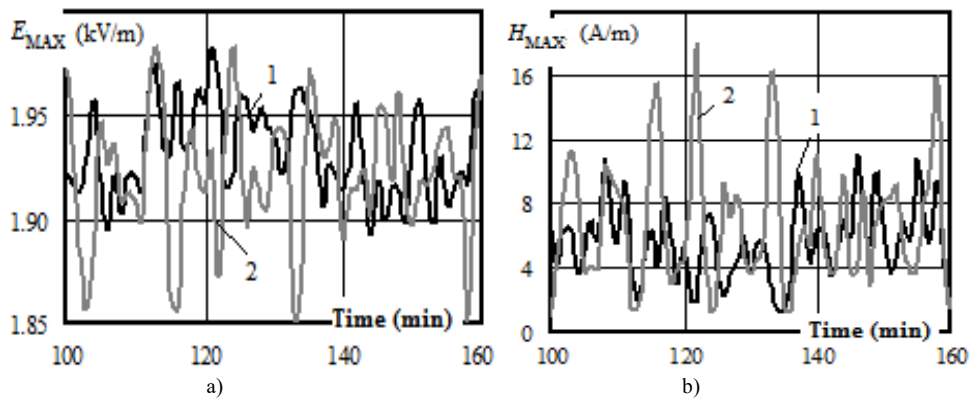


Fig. 8. EMF dynamics in the point with coordinates $X = 3$ m, $Y = 1,8$ m: a – electric field, b – magnetic field.

Table 3. EMF values at various train schedules, $X = 3$ m, $Y = 1,8$ m.

Indicator	E _{MAX}		H _{MAX}		Difference of columns 2 & 3	Difference of columns 4 & 5
	Schedule 1	Schedule 2	Schedule 1	Schedule 2		
1	2	3	4	5	6	7
Average	1,96	1,95	3,45	4,19	0,28	-21,6
Maximum	2,00	2,00	11,0	18,0	0,00	-62,8
RMSD	0,02	0,03	2,96	4,16	-32,7	-40,4

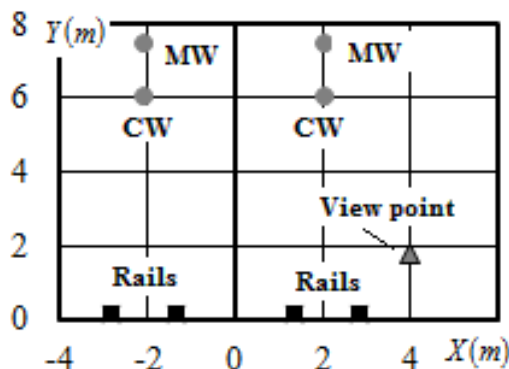
Another possibility of minimizing the magnetic field of the traction network is associated with the choice of the mode of train operation. For freight trains, different types of locomotives and different modes of train operation can be used, depending also on the individual characteristics of the drivers. With the limited power of the locomotive, the mode of train operation is forced to be "soft", with limited power consumption, without sharp jerks and with limited speed. With sufficient power of electric locomotives leading the train "hard" mode of operation is quite possible, in which the maximum traction with large power consumption alternates with the run-up with low power consumption. In this variant the voltage in the contact network is significantly reduced and the current consumed by the train increases, which in turn leads to an increase in the magnetic field strength created by the traction network.

To assess the different impacts of the modes of train operation on the electromagnetic situation, EMF of one of the main railways of Eastern Siberia was simulated. The complete scheme included 845 nodes and 4,896 branches, simulating a two-track section with a PBSM-95+MF-100 catenary system of each track 1,300 km long. The design section included 29 traction substations with transformers TDTNZh-40000/230 powered from the two-circuit 220 kV line. The traffic schedule was made for down trains weighing 3,200 tons and an up trains weighing 6,000 tons with 35-minute intervals between trains.

The results of calculating the magnetic field at a point with coordinates $X = 4$ m, $Y = 1,8$ m based on fig. 9 are presented in table 4 and in fig. 10 - 12.

Table 4. Maximum and middle values of magnetic field amplitude (A/m).

#	Parameter	Regime		Difference, %
		Soft	Hard	
1	Average value	13,25	15,58	15
2	Maximum	23,10	30,79	25

**Fig. 9.** Wires coordinates and view point coordinates: CW – contact wire; MW – messenger wire.

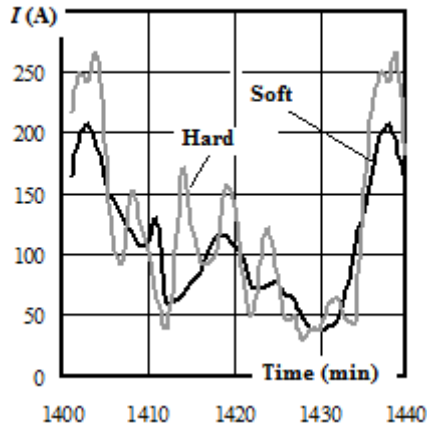


Fig. 10. Contact net current dynamics at the beginning of control section.

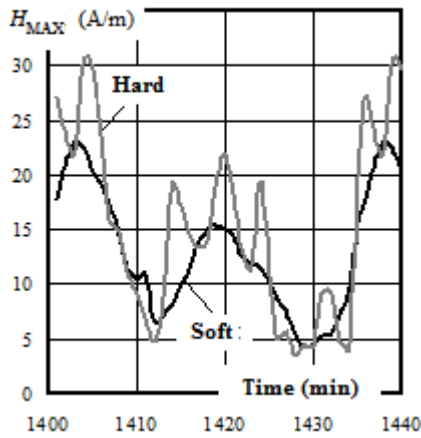


Fig. 11. Magnetic field dynamics at the beginning of control section.

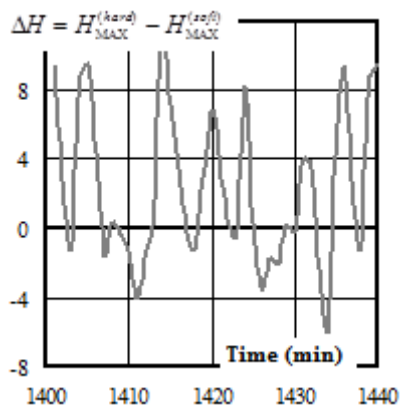


Fig. 12. Magnetic field differences of hard and soft train voving.

Thus, the use of "soft" modes of train operation can reduce the maximum value of the magnetic field by about 25%, and the average value of the voltage during the observation period by 15%.

5 Conclusion

1. The control of the electromagnetic situation on the railroad can be reduced to the task of decreasing the levels of magnetic field strength at given points of space, which surrounds the traction network. Methods for solving this problem are divided into technical and regime ones. The technical measures include the following: application of autotransformer 2 -25 kV RPSSs; use of booster transformers with return wire; mounting of reinforcing and shielding wires; use of passive screens installed on passenger platforms. The regime measures include the optimization of traffic schedules and modes of train operation by the criterion of improving the EMS, as well as the application of the systems of train automatic operation with algorithms aimed at reducing peak loads.
2. The intensity of magnetic field can be reduced through the use of optimal train schedules, as well as using the "soft" modes of train operation. The latter measure is able to reduce the peak magnetic field strength by about 25%.

References

1. M. Bernd, A. Zbigniew, *Smart Grids – Fundamentals and Technologies in Electricity Networks* (Springer, Verlag Berlin Heidelberg, 2014)
2. S.M. Apollonsky, *Problems of electro-magnetic safety on electrified railway*. (RUSAINS, Moscow, 2017)
3. V.P. Zakaryukin, A.V. Kryukov, et.al. The power grid of the future **2**, 39-44 (2013)
4. A. Steimel, *Electric traction motive power and energy supply. Basics and practical experience* (Oldenbourg Industrieverlag, Munchen, 2008)
5. H. Biesenack, E. Braun, G. George, *Energieversorgung elektrischer bannen* (Wiesbaden, Verlag, 2006)
6. A. Ogunsola, A. Mariscotti, *Electromagnetic Compatibility in Railways* (Springer, 2013)
7. A. Ogunsola, U. Reggiani, L. Sandrolini, Modelling Electromagnetic Fields Propagated from an AC Electrified Railway Using TLM **EMC09**, 567-570 (2009)
8. R.J. Hill, Transactions on the Built Environment **6**, 383-390 (1994)
9. M. Mandić, I. Uglešić, V. Milardić Tehnički vjesnik **20(3)**, 505-509 (2013)
10. V.P. Zakaryukin, A.V. Kryukov, Innovation & Sustainability of Modern Railway – Proceedings of ISMR'2008, China Railway Publishing House, 504-508 (2008)
11. J.A. Stretton, *Electromagnetic theory* (McGraw-Hill co., New York, 1941)
12. S.M. Apollonsky, A.N. Gorsky, *Calculations of electromagnetic fields* (Marshrut, Moscow, 2006)
13. L.R. Neuman, K.S. Demirchian, *Theoretical foundations of electrical engineering* (Vysshaya Shkola, Moscow, 1981)
14. R.A. Katz, L.S. Perelman, *Electrichestvo* **1**, 16-19 (1978)
15. M. Milivoj, U. Ivo, V. Milardić, Technical Gazette **20(3)**, 505-509 (2013) ISSN 1848-6339